Physical properties of petroleum formed during maturation of Lower Cambrian shale in the upper Yangtze Platform, South China, as inferred from PhaseKinetics modelling

ARTICLE *in* MARINE AND PETROLEUM GEOLOGY · DECEMBER 2013

Impact Factor: 2.64 · DOI: 10.1016/j.marpetgeo.2013.07.013

Marine and Petroleum Geology 48 (2013) 47–56

Contents lists available at ScienceDirect

Marine and Petroleum Geology

journal homepage: www.elsevier.com/locate/marpetgeo

Physical properties of petroleum formed during maturation of Lower Cambrian shale in the upper Yangtze Platform, South China, as inferred from PhaseKinetics modelling

Jingqiang Tan [a,*], Brian Horsfield [a], Nicolaj Mahlstedt [a], Jinchuan Zhang [b], Rolando di Primio [a], Thi Anh Tiem Vu [a], Christopher J. Boreham [c], Ger van Graas [d], Bruce Alastair Tocher [d]

[a] GFZ – German Research Centre for Geosciences, Potsdam 14473, Germany
[b] China University of Geosciences (Beijing), Beijing 100083, China
[c] Geoscience Australia, GPO Box 378, Canberra 2601, ACT, Australia
[d] Statoil, Oslo, Norway

ARTICLE INFO

Article history:
Received 22 January 2013
Received in revised form
28 June 2013
Accepted 22 July 2013
Available online 1 August 2013

Keywords:
Lower Cambrian shale
South China
Shale gas
Petroleum generation
PhaseKinetics
Phase behaviour

ABSTRACT

Lower Cambrian shale in the Upper Yangtze Platform (UYP), South China, is an important source rock of many conventional petroleum fields and was recently recognized as a promising unconventional shale reservoir. In this paper, hydrocarbon generation kinetics and petroleum physical properties were investigated using the PhaseKinetics approach (di Primio and Horsfield, 2006) and a Cambrian shale sample from the Georgina Basin, North Territory Australia (NTA), as similar paleogeological and sedimentary environments in Cambrian are found for the UYP and NTA.

The source rock comprises type II kerogen and belongs to an organofacies generating Paraffinic–Naphthenic–Aromatic low wax oil. Bulk petroleum generation can be described by a single frequency factor $A = 8.43E + 14$ (1/s) and a dominant activation energy at 56 kcal/mol, which is characteristic for sulphur-poor organic matter deposited in an anoxic marine environment. Onset (transformation ratio $TR = 10\%$) and end ($TR = 90\%$) of bulk hydrocarbon generation was calculated to take place at 120 °C and 165 °C respectively for an assumed average geological heating rate of 1.5°C/Ma. Based on the thermal history of a local "model"-well, onset temperature was not reached until the Middle Triassic (241 ma) when sediments were buried more than 2000 m and basalt eruptions caused enhanced heat flows. The main generation stage of primary petroleum took place during the Middle–Late Triassic and ended in the Early Jurassic (187 ma) for burial depths exceeding 4000 m (*TR* 90%; 165 °C). Temperatures increased to more than 200 °C in the Middle–Late Jurassic leading to secondary cracking of primary products.

Hydrocarbons formed at the onset ($TR = 10\%$) of petroleum generation can be characterized by a gas-oil-ratio (*GOR*) of 63 Sm^3/Sm^3, a saturation pressure (P_{sat}) of 101 bar, and a formation volume factor (B_o) of 1.2 m^3/Sm^3. Those parameters stay low during primary petroleum generation before 203 ma, at temperatures < 145 °C, and at burial depths <3400 m (*GOR* = 176 Sm^3/Sm^3, $P_{sat} = 189$ bar, $B_o = 1.6$ m^3/Sm^3 at 90% *TR*). However, predicted parameters increase rapidly (*GORs* >> 10,000 Sm^3/Sm^3, $P_{sat} > 250$ bar and $B_o > 2.0$ m^3/Sm^3) during secondary cracking starting roughly at 200 ma, 152 °C and 3500 m burial. Assuming zero expulsion, the shale reservoir position within the sedimentary basin indicates that bubble point pressure was always below reservoir pressure, and fluids in the shale reservoir occurred only as a single, undersaturated phase throughout maturation history. Black oil and volatile oil phases dominated during the primary cracking period, whereas wet gas and dry gas phases dominated during the secondary cracking period.

1. Introduction

In China, the Upper Yangtze Platform (UYP) is one of the major conventional petroleum producing regions, with annual natural gas production accounting for 22–43% of the total national production

* Corresponding author. Tel.: +49 331 288 28688.
E-mail address: Jqtan@gfz-potsdam.de (J. Tan).

0264-8172/$ – see front matter © 2013 Elsevier Ltd. All rights reserved.
http://dx.doi.org/10.1016/j.marpetgeo.2013.07.013

in the last 20 years (National Bureau of Statistics and Energy Bureau, 1991–2010). Petroleum reservoirs are predominantly composed of the Changxing (Upper Permian) and Feixianguan (Lower Triassic) carbonates and the Xujiahe (Upper Triassic) and Jurassic terrigenous clastics, which accounted for over 70% of total reserves (Dai et al., 2009; Ma et al., 2010). Prolific source rocks are the Lower Cambrian, Lower Silurian and Lower Jurassic mud shales, the Lower Permian carbonate, as well as Upper Permian and Upper Triassic coal-bearing shales. Regional seals are mainly consisting of anhydrite, halite, and gypsiferous dolomite that developed in a major marine regression between the Late Early and Middle Triassic (Editorial Committee Division of Sichuan Oil & Gas field, 1989; Dai et al., 1992; Huang et al., 1997; Jia et al., 2006; Ma et al., 2006, 2010; Hao et al., 2008).

As an important regional source rock for many petroleum fields in the Yangtze Platform, Lower Cambrian shales are distributed almost throughout the whole area (Fig. 1). In the UYP, Lower Cambrian shales usually possess thicknesses between 100 and 200 m in the south and north Sichuan Basin, west Hunan and Hubei Province, and north Guizhou and Yunnan Province (Fig. 1). In the central Sichuan Basin and the west and south marginal areas of the UYP Lower Cambrian shales are only very thin if present at all. In regions, where thick shale successions predominate, higher average TOC contents >2%, are encountered (Cheng et al., 2009; Liang et al., 2009). Present organic matter is generally overmature with vitrinite reflectances between 2.0 and 4.0%, and values increasing from west to east (Zhang et al., 2008; Wang et al., 2009a, 2009b).

In addition to its importance for conventional petroleum production, Lower Cambrian shale has only recently been recognized as a prolific unconventional resource play (EIA, 2011). The shale distribution (extent, depth and thickness), sedimentary environment, organic matter richness, thermal maturity, and mineralogical composition can be compared to the Barnett Shale (Zhang et al., 2008; Cheng et al., 2009; Dong et al., 2010; Zou et al., 2010, 2011; Long et al., 2012), which is often used as an exploitation model.

In both conventional and unconventional petroleum systems, it is important to reconstruct the timing of petroleum generation as well as the changing *GOR* of the petroleum and its physical properties during maturation. The timing and extent of petroleum generation depends on both the thermal history of the source rock and the reaction kinetics of hydrocarbon generation from kerogen (Behar et al., 1997). Kinetic laws are therefore routinely considered as a very critical element in the modelling of hydrocarbon generation from source rocks (Tegelaar and Noble, 1994; Dieckmann et al., 1998). Kinetic parameters of petroleum generation from kerogen are usually derived by pyrolysis of immature source rocks. In the case of UYP, unfortunately, all published data as well as our own Rock-Eval and Open-System Thermal Analysis GC-FID results shows that Lower Cambrian shale in the UYP is overmature, and therefore reconstructing the entire petroleum generation history is fraught with difficulty. Here we report how we overcame this problem by using comparable immature samples from Australia. Specifically, Cambrian shale from the Georgina Basin, Northern Territory of Australia was selected because of its paleo-geological and -tectonic position close to the South China Plate throughout the Paleozoic.

2. Selection of Cambrian geological analogue

Stratigraphic correlations and tectonic analysis indicate that the Yangtze plate of South China can be viewed as a continental fragment caught between the Australian craton and Laurentia during the late Mesoproterozoic assembly of the supercontinent Rodinia (Li et al., 1995). Although the breakup of Rodinia around 0.7 Ga separated South China (Yangtze plus Cathaysia plates) from the other continents, the South China Plate remained adjacent to North Australia for a very long geological time, which lasted throughout the whole Paleozoic (Fig. 2) (Scotese and McKerrow, 1990; Scotese,

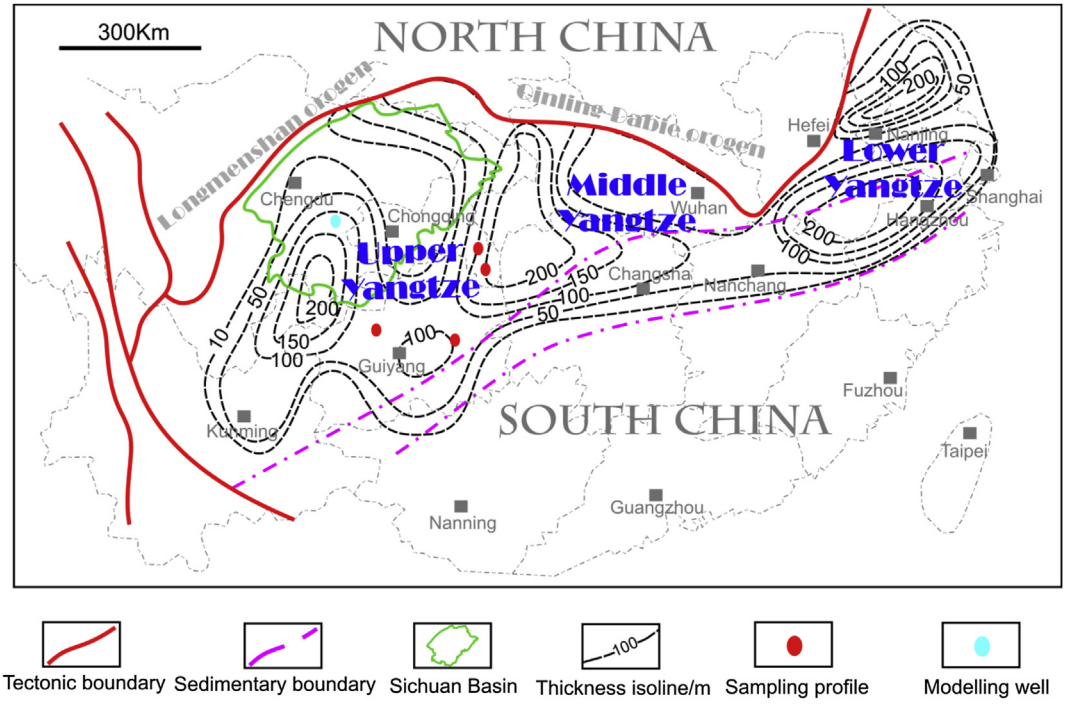

Figure 1. Lower Cambrian shale distribution in the Yangtze Platform, modified after (Liang et al., 2008; Zou et al., 2011).

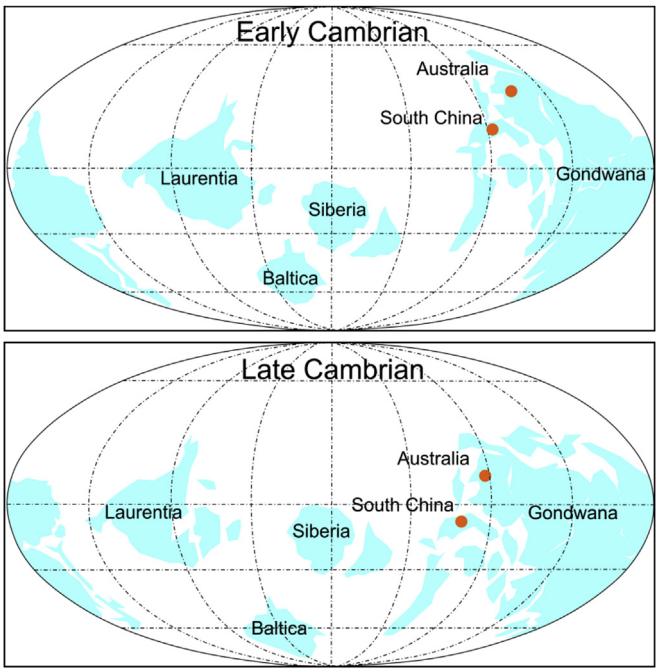

Figure 2. Paleocontinents in the Cambrian: red points indicate locations of South China and North Australia, modified after (Scotese and McKerrow, 1990). (For interpretation of the references to colour in this figure legend, the reader is referred to the web version of this article.)

2009). The Precambrian-Paleozoic geology of the Yangtze Plate has therefore already been linked to Australian geology (Li et al., 2003; Steiner et al., 2007), where similar shallow sea sedimentary environments occurred in the Cambrian (Scotese, 2009).

2.1. Cambrian geology – UYP

Tectonically, the UYP comprises the western part of the Yangtze Platform in South China and is enveloped by the Longmenshan orogen in the west and the Qinling–Dabie orogen in the north (Korsch et al., 1991; Meng et al., 2005; Jia et al., 2006; Plesch et al, 2007). It regionally includes the eastern Sichuan, Chongqing area, most of Guizhou, western Hubei and Hunan, and northern Yunnan province. The Tongwan tectonic movement occurring at the end of the Proterozoic resulted in a disconformity between the upper Proterozoic (Sinian) and the Lower Cambrian. The Early Cambrian succession consists of carbonaceous and calcareous shale, carbonate, siltstone and fine stone and was deposited in a major marine transgression from Southeast to Northwest. The black shale is thickening from northwest to southeast, therefore, the present South and North Sichuan, western Hunan and Hubei, Chongqing and Guizhou contain thick black shale successions deposited in an open marine platform to marine shelf environment, whereas the present western marginal area is predominated by clastics and carbonates which were deposited in littoral environments. In the Middle–Late Cambrian, the open marine platform and marine shelf environments were maintained in the western Hunan and Hubei, while in other places a mainly restricted marine platform environment resulted from a regression. Thick Cambrian carbonates were deposited extensively, whose total original thickness would be higher than 2000 m in the south and east UYP if no erosion had resulted from the Late Caledonian Uplift (Editorial Committee Division of Sichuan Oil & Gas field, 1989; Korsch et al., 1991; Ma et al., 2007; Hao et al., 2008). In the Sichuan Basin, Lower Cambrian Shale was recognized as one of the major source rocks for many reservoirs, such as the Weiyuan gas field besides others in the eastern part of the basin (Ma et al., 2007, 2010; Dai et al., 2009). Meanwhile, the Middle–Late Cambrian carbonate has good petroleum reservoir characteristics (Editorial Committee Division of Sichuan Oil & Gas field, 1989).

2.2. Cambrian geology – Georgina Basin

The Georgina Basin covers an area of >100,000 km^2 and is the largest Neoproterozoic–Paleozoic intracratonic basin in Australia. It evolved after the breakup of the Centralian Superbasin in the Late Neoproterozoic (Haines et al., 2001; Volk et al., 2007). The present outline is an erosional remnant of a much larger, Vendian-lower Paleozoic sedimentary package, deposited in sub- to supratidal environments across parts of an epicontinental shelf that covered large tracts of central and northern Australia. Cambrian organic-rich shales in the Thorntonia Limestone, Arthur Creek formation and Chabalowe formation provide important source rocks as well as contain the main reservoir targets in the basin. In early Cambrian, the southern basin margin was restricted. Lower Cambrian siliciclastic rocks and carbonates were deposited and unconformably overlay the Neoproterozoic Elkera Formation with a total thickness of almost 250 m. To Middle Cambrian, sedimentation recommenced during a major transgression and resulted in peritidal to restricted, shallow marine environments and the deposition of the Thorntonia Limestone. Following basin-wide erosion and the formation of a regional unconformity, deepening marine conditions resulted in the deposition of anoxic, pyritic and carbonaceous, partly dolomitic shale of the basal, up to 60 m thick Arthur Creek formation acting as the main source rock unit. A thick Late Cambrian succession of mixed peritidal carbonate rocks and redbeds of the Chabalowe Formation was deposited in an extensive and intermittently emergent epeiric sea. The basal Hagen Member deposited mainly in the southwest, comprises reservoir-quality dolostone, with subordinate grainstone at the base, overlain by massive anhydrite, which acts as a seal. The Chabalowe Formation is in turn overlain by carbonate and siliciclastic rocks of the Arrinthrunga Formation (Ambrose and Putnam, 2005; Boreham and Ambrose, 2007).

3. Selection of shale samples

3.1. Lower Cambrian shale samples from UYP

Organic richness, maturity, kerogen type as well as free hydrocarbons and kerogen quality have already been assessed for fifteen samples collected from four Lower Cambrian shale profiles throughout the Chongqing area and Guizhou province (Fig. 1). Results are described in detail in Tan et al. (2013) and can be summarized as follows. The TOC content in many profiles ranges between 5 and 10% with the organic matter itself being overmature ($R_o >> 2\%$). This causes very low residual-genetic potentials precluding the direct identification of original kerogen type. Previous researches suggested a mixed type I/II alginitic/bacterial kerogen leading to Lower Cambrian shale being viewed as an important source rock in the UYP (Liang et al., 2009; Zou et al., 2010).

3.2. Lower Cambrian shale sample from the Georgina Basin, North Australia

The basal Arthur Creek Fm. is up to 60 m thick and comprises mainly algal/bacterial (type I/II kerogen) organic matter with TOC contents in the range of 0.5–16% and HIs higher than 600 mg HC/g TOC (Ambrose et al., 2001; Ambrose and Putnam, 2005; Volk et al., 2007). An immature core sample (HI = 601 mg/g TOC, TOC = 15.8%,

$T_{max} = 428$ °C) taken from a depth of 107 m of a well located in the southern Georgina Basin was therefore chosen as a source rock equivalent for Lower Cambrian Shales in the central UYP.

4. Analytical and modelling methods

PhaseKinetics is a compositional kinetic modelling method that is based on pyrolysis gas chromatography to establish Petroleum Type Organofacies, bulk flow pyrolysis to determine bulk petroleum generation parameters, MSSV pyrolysis to determine bulk compositions at selected Transformation Ratios, and finally, tuning to configure results in a PVT-amenable format. Here we perform this workflow on an Australian sample, and then apply the results in a 1-D petroleum system model of a local well within the UYP.

4.1. Open-system pyrolysis gas-chromatography (open-Py)

Pyrolysis gas chromatography was performed on the immature whole rock sample from Georgina Basin using the Quantum MSSV-2 Thermal Analysis System© interfaced with an Agilent GC-6890A (Horsfield et al., 1989). About 30 mg sample was placed into the central part of a glass tube (26 mm long, inner sleeve diameter 3 mm). The remaining volume was filled with purified quartz that had been cleaned by heating at 630 °C in fair of 30 min. The sample was heated in a flow of helium, all products released up to 300 °C being vented (3 min, isothermal). After then, it was pyrolysed at 50 °C/min from 300 to 600 °C and pyrolysis products were collected in a cryogenic trap (liquid nitrogen cooling at −190 °C, glass beads substrate) for condensation, from which they were later liberated by ballistic heating (held at 300 °C for 10 min). AHP-Ultra 1 dimethylpolysiloxane capillary column (50 m length, inner diameter of 0.32 mm, film thickness of 0.52 mm) connected to a Flame-Ionisation-Detector (FID) was used with helium as carrier gas. The GC oven temperature was programmed from 30 °C to 320 °C at 5 °C/min. Boiling ranges (C_1, C_{2-5}, C_{6-14}, and C_{15+}) and individual compounds (*n*-alkenes, *n*-alkanes, alkylaromatic hydrocarbons and alkylthiophenes) were quantified by external standardisation using n-butane. Response factors for all compounds were assumed the same, except for methane whose response factor was 1.1.

4.2. Bulk kinetics

Kinetic parameters of primary kerogen to petroleum conversion were assessed by subjecting the same sample to open-system, non-isothermal pyrolysis at four different linear heating rates (0.7, 2, 5, 15 °C/min) using a Source Rock Analyser SRA (Humble). Roughly 100 mg of crushed sample material was weighed into small vessels and heated according to the temperature program from 250 °C to ~600 °C. Generated bulk products were transported to the FID in a constant helium flow of 50 ml/min. The discrete activation-energy (Ea) distribution optimization with a single, variable frequency factor (A) was performed using the KINETICS05 and KMOD® programs (Burnham et al., 1987).

4.3. Closed-system pyrolysis gas-chromatography (MSSV-Py)

Non-isothermal closed-system micro-scale-sealed-vessel (MSSV-) pyrolysis gas chromatography (principles described in Horsfield et al., 1989) was employed to obtain compositional information on petroleum products as input parameter for phase kinetic modelling. Ca. 20 mg of finely ground, whole rock was weighed into glass capillaries, which were then sealed by an H_2-flame after reducing the internal volume of the tube from ca. 40 ml to ca. 15 ml with pre-cleaned quartz sand. Pyrolysis was performed off-line at 0.7 K/min to temperatures corresponding to 10, 30, 50, 70, and 90% *TR* as defined by bulk pyrolysis (SRA), using an external high performance oven. The latter consisted of a massive cylindrical metal block acting as a circular sample holder enclosing a central heating cartridge, which provided a very homogeneous temperature field throughout the core. Excellent temperature control was guaranteed by a thermocouple introduced directly into one sample holder. After removal from the external pyrolysis oven, samples were introduced into the Quantum MSSV-2 Thermal Analyzer pyrolysis oven unit interfaced with an Agilent GC 6890A apparatus equipped with an HP-Ultra 1 column of 50 m length, 0.32 mm internal diameter and 0.52 mm thickness and an FID. The tubes were purged 5 min at 300 °C to remobilize generated products and then cracked open by a piston device to transfer generated products from within the vessel by a helium-carrier gas with a flow rate of 30 ml/min into a liquid nitrogen-cooled trap. The trapped hydrocarbons were released to the column by ballistic heating of the trap to 300 °C. The GC oven temperature was programmed from 30 °C to 320 °C at 5 °C/min. Quantification of individual compounds and totals was conducted by external standardisation with *n*-butane. Reproducibility of measured product concentration is generally better than 4% (Schenk et al., 1997). Because of the lower response factor of methane compared to the heavier gases the methane content was multiplied by 1.1.

4.4. Compositional kinetic modelling

Having acquired bulk kinetic parameters (activation energy-Ea and frequency factor-A) of primary petroleum formation and the composition of generated hydrocarbons at 10, 30, 50, 70, and 90% kerogen conversion, a compositional kinetic model for the prediction of hydrocarbon physical properties (*GOR*, P_{sat}, *Bo*) under subsurface conditions could be determined using the PhaseKinetics approach established by di Primio and Horsfield (2006). *GOR* is the gas oil ratio, which is the ratio of total gas hydrocarbons (C_{1-5}) and total liquid hydrocarbons (C_{6+}) at standard surface conditions (Sm^3/Sm^3). Bo is the formation volume factor, which is the ratio of reservoir liquid volume to surface liquid volume in m^3/Sm^3. P_{sat} is the saturation pressure, the pressure which occurs when oil cannot dissolve any more gas.

As gas composition dominantly controls petroleum phase behaviour, and laboratory pyrolysis results in less dry composition than field data implies, a gas composition correction was performed as described in (di Primio et al., 1998). For basin modelling purposes and assuming a heating rate of 1.5°C/ma, results were applied to the geological evolution of Cambrian shale within a selected synthetic well located in the UYP (central-south Sichuan Basin; 30.00N; 105.40E).

4.5. 1-D petroleum system modelling

A synthetic well located in the central-south Sichuan Basin, UYP (Fig. 1), was selected for applying the PhaseKinetics model using 1D modelling (Fig. 3). Lower Cambrian shale is overlying Upper Sinian carbonate, and is covered by Paleozoic carbonate and shale and Mesozoic sandstone and shale. There are three shale formations respectively in the Lower Cambrian, Upper Permian and Upper Triassic succession. The deepest burial depth of Lower Cambrian shale was close to 6000 m with maximum temperatures around 220 °C in the Late Jurassic. At present, the depth and temperature of this formation near the well ranges from 4600 to 4900 m and 140 °C to 160 °C (Wang et al., 2009a; Xu et al., 2011). Three major uplift and erosion periods occurred from the end of the Silurian to Carboniferous, during the Late Permian, and from Cretaceous to present times. During burial, the Lower Cambrian Shales within the well in the Sichuan Basin experienced relative slow heating rates

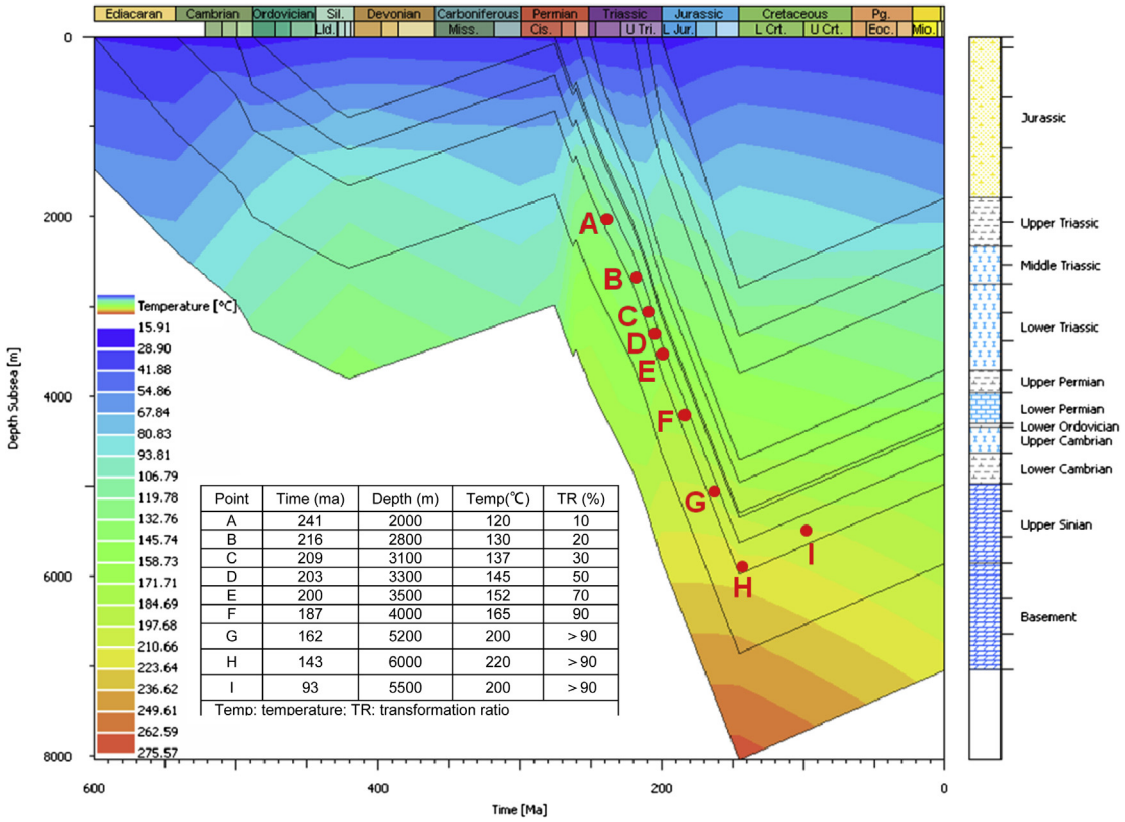

Figure 3. 1D results in central-south Sichuan Basin, UYP. Reservoir conditions of the Lower Cambrian shale represented by red points are respectively: A – 2000 m, 241 ma, and 120 °C; B – 2800 m, 216 ma, and 130 °C; C – 3100 m, 209 ma, and 137 °C; D – 3300 m, 203 ma, and 145 °C; E – 3500 m, 200 ma, and 152 °C; F – 4000 m, 187 ma, and 165 °C; G – 5200 m, 162 ma, and 200 °C; H – 6000 m, 143 ma, and 223 °C; I – 5500 m, 93 ma, and 200 °C. (For interpretation of the references to colour in this figure legend, the reader is referred to the web version of this article.)

between 1 and 2°C/ma, only accelerated by the Emeishan magmatic activity in Middle–Late Permian times (Zhu et al., 2010). A continuous, long period of subsidence commenced in the Permian and continued until the Late Jurassic. Here and which will be shown in the following in more detail, primary hydrocarbon generation most likely occurred, i.e. between the Middle Triassic and Early Jurassic.

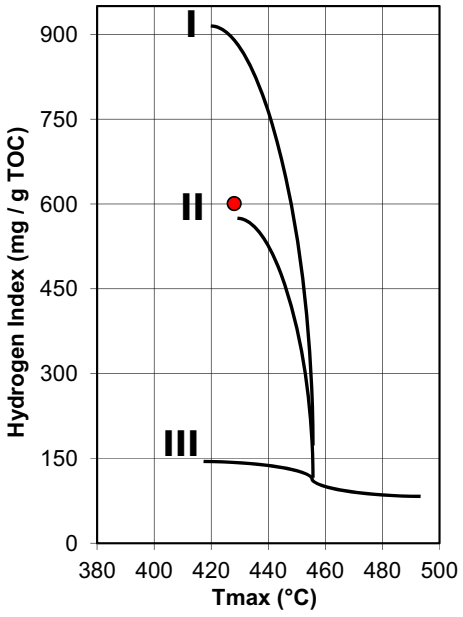

Figure 4. OI versus HI.

5. Results and discussions

5.1. Petroleum type organofacies

The sample from the Georgina Basin has a very high petroleum potential (HI = 601 mg/g TOC), and comprises type II kerogen (Espitalié et al., 1984) (Fig. 4). Pyrolysis products are dominated by light hydrocarbons and show a notable presence of 1, 2, 3, 4-tetramethylbenzene (Fig. 5), which is suggestive of photic zone euxinia during deposition (Hartgers et al., 1994; Muscio et al., 1994; Wanglu et al., 2007). In Figure 6 a paraffinic–naphthenic–aromatic low wax oil petroleum type can be inferred (Horsfield, 1989), but with a pyrolysate composition very close to the boundary of the gas condensate petroleum type organofacies field (Fig. 6). The ability of marine source rocks to generate anomalously high amounts of light hydrocarbons could be an important characteristic of high quality gas shales in general.

5.2. Bulk maturation characteristics

Bulk kinetic parameters for primary kerogen conversion are given in Table 1 and Figure 7. Hydrocarbon generation can be described by a single frequency factor of $A = 8.429E + 14$ 1/sec and an activation energy distribution ranging from 44 to 67 kcal/mol. The main activation energy at 56 kcal/mol, accounting for 36.5% of

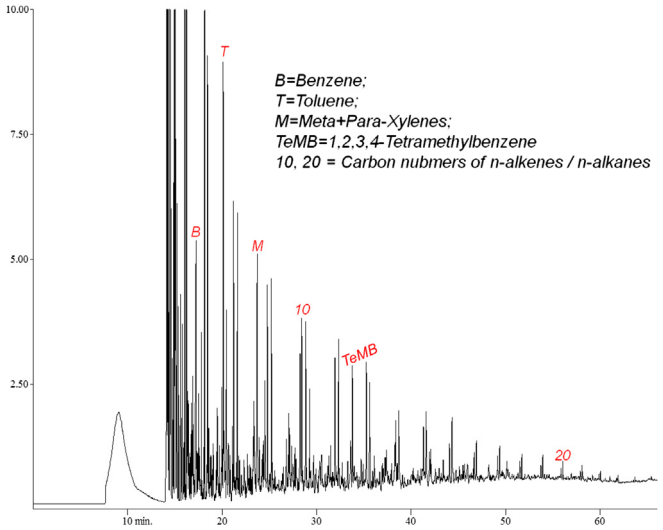

Figure 5. Pyrolysis gas chromatogram of the sample from Georgina Basin.

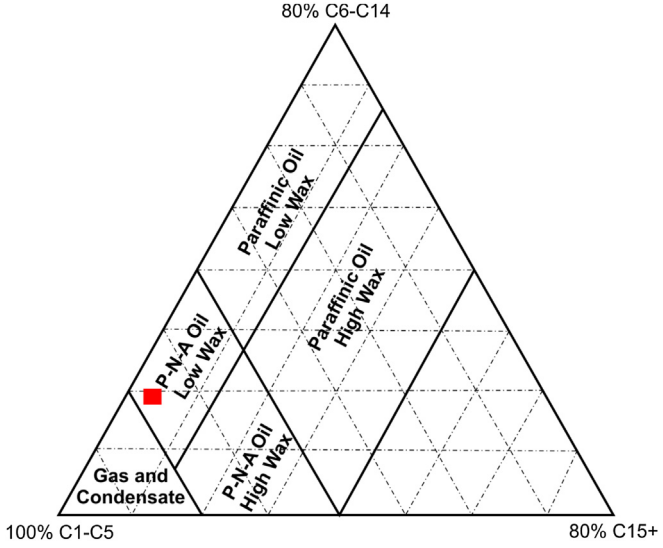

Figure 6. Petroleum type organofacies.

the bulk reaction, is higher than commonly assumed for oil and gas formation from marine, clastic source rocks. Compared to type II model source rocks (51–54 kcal/mol) (Braun and Burnham, 1992), Jurassic Posidonia Shale (52–54 kcal/mol) (Dieckmann et al., 1998), or a series of sample from different facies (48–55 kcal/mol) investigated by di Primio and Horsfield (2006), organic matter within the old Cambrian shale shows higher stabilities than organic matter within younger ones (Devonian to Mesozoic source rocks). Extrapolation to a geological heating rate of 1.5 °C/ma, which fits the averagely experienced thermal stress of Lower Cambrian shale in the UYP, indicates an onset temperature of hydrocarbon generation ($TR = 10\%$) near 120 °C, while the end of generation ($TR = 90\%$) can be expected for temperatures around 165 °C (Fig. 8). The latter prediction is characteristic for marine but sulphur-poor organic

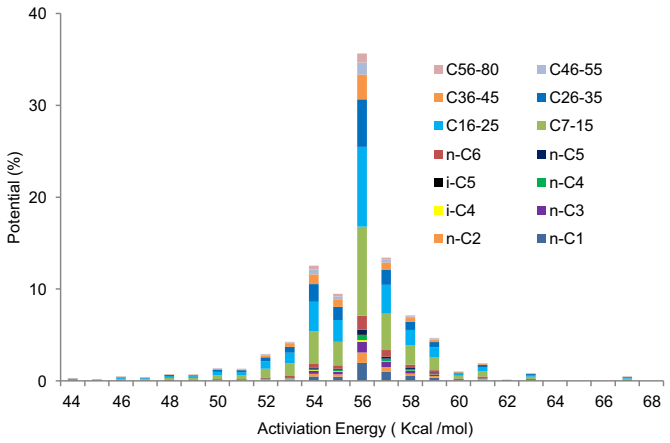

Figure 7. Activation energy distribution populated by MSSV data.

matter if compared the data of Tegelaar and Noble (1994) or di Primio and Horsfield (2006).

5.3. Compositional kinetics

The activation energy distribution populated by MSSV data is given in Figure 7. The gases are predominated by n-C_1, n-C_2 and n-C_3, while liquids are predominated by lumped boiling ranges C_{7-15} and C_{16-25}. The influence of the measured and corrected petroleum composition on the physical properties of the primary formed fluid is displayed in Figure 9 in which the evolution of *GOR*, P_{sat} and B_o as a function of maturity, defined by *TR*s, is shown. For *TR*s between 10 and 90% *GOR* ranges between 63 and 176 Sm^3/Sm^3, P_{sat} ranges between 101 and 189 bar, and B_o ranges between 1.2 and 1.6 m^3/Sm^3, respectively. Thus, black oil (*GOR*s up to 200 Sm^3/Sm^3) is generated throughout primary kerogen conversion, which might be secondarily cracked to gas in-source or in-reservoir. As high thermal maturities are reached for Lower Cambrian Shale in the UYP, modelled evolution of *GOR*s including secondary composition are displayed in Figure 10 for an assumed heating rate of 1.5 °C/ma as a function of temperature. It can be deduced from rapidly increasing *GOR*s that secondary cracking starts at temperatures close to 150 °C, whereas primary hydrocarbon generation proceeds up to 165 °C (compare Fig. 8 *TR* 90%). This means that secondary cracking starts when *TR* reaches ~60%, i.e. before primary cracking of kerogen is completed. In Figure 11 the predicted relationship between P_{sat} and B_o for Lower Cambrian shale in the UYP (pink line), with P_{sat} increasing from 101 to 300 bar and B_o increasing from 1.2 to 2.3 m^3/Sm^3 for increasing maturity levels, is compared to measurements on hundreds of samples from the Northern Sea, Norway. The fluid properties evolution curve seems to fit the natural case very well, with black oil being generated at low mature stages and gas condensates at overmature stages when secondary cracking predominates.

5.4. Petroleum phase behaviour prediction in the UYP

Petroleum phase behaviour of fluids potentially generated during maturation of the UYP Cambrian shale was defined for the

Table 1
Bulk kinetics parameters of total hydrocarbon potential (%), frequency factor $A = 8.429E + 14$ (1/s).

Ea(kcal/mol)	44	45	46	47	48	49	50	51	52	53	54	55	56	57	58	59	60	61	62	63	64	65	66	67
Fraction(%)	0.25	0.15	0.41	0.33	0.64	0.62	1.18	1.15	2.53	3.67	12.01	9.59	36.50	14.05	7.46	4.91	1.07	2.03	0.09	0.87	0.00	0.00	0.00	0.49

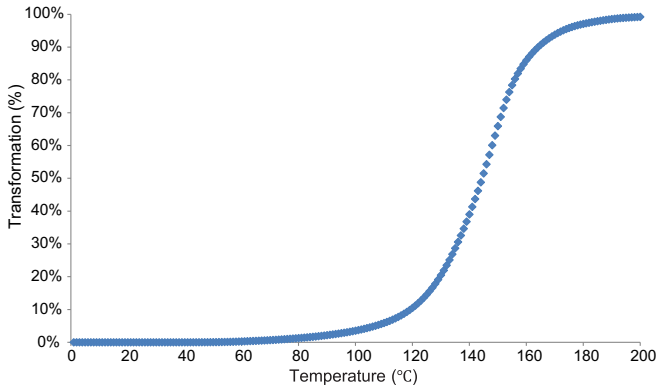

Figure 8. Predicted *TR* evolution with a function of temperature for a heating rate of 1.5 °C/ma.

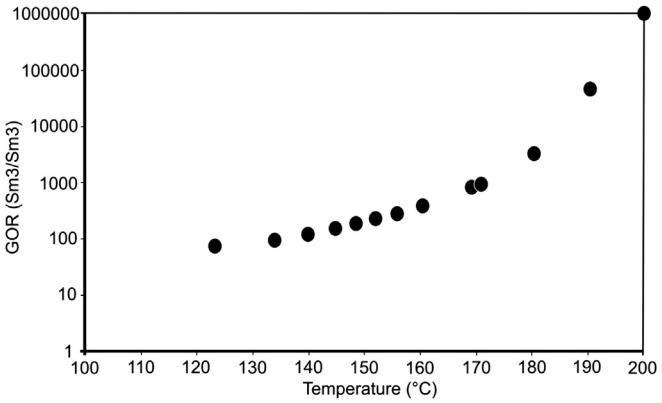

Figure 10. Predicted *GOR* evolution with a function of temperature for a heating rate of 1.5 °C/ma.

temperatures 120, 130, 137, 145, 152 and 165 °C (Fig. 12), which are respectively corresponding to 10, 20, 30, 50, 70 and 90% *TR* (Fig. 8). For the present case study it is assumed that all products are retained in the shale reservoir and nothing is expelled. Reservoir pressure applied in the model was calculated only based on the reservoir depths in Figure 3 (red points, A–F) and assuming a geopressure gradient of 100 bar/km.

Subsequent to basalt eruption in Permian, the onset of primary hydrocarbon generation occurred in the Middle Triassic (241 ma) at a burial depths around 2000 m (Fig. 3). Here and as shown in Figure 12A, the phase envelope of the generated fluid indicates petroleum with a *GOR* lower than 100 Sm^3/Sm^3 (compare Fig. 10) and a bubble point pressure (P_b) around 120 bar, which is much lower than the shale reservoir pressure (P_r). The bubble point pressure P_b corresponds to the pressure for which gas dissolves from the oil phase. The generated black oil (*GOR* < 200 Sm^3/Sm^3 in Fig. 10) therefore existed as a single oil phase at shale reservoir conditions. In the case of expulsion of this undersaturated black oil and migration into overlying strata in which lower reservoir pressures existed, a 2-phase system would be reached at 120 bar. Based on the kinetics black oil generation continued to the Late Triassic (203 ma) for burial depths up to 3300 m and temperatures around 145 °C (Figs. 3 and 12D). In that period, although P_b has increased to over 260 bar, the shale reservoir pressure P_r was still much lower.

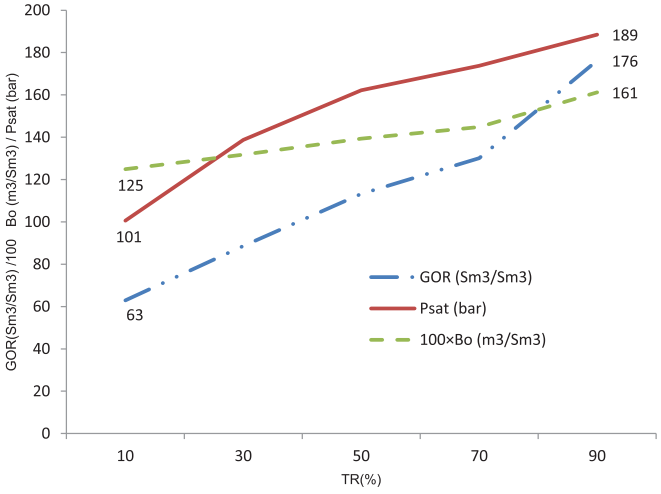

Figure 9. Calculated *GOR*, P_{sat}, B_o evolution with a function of *TR*.

Thus, petroleum occurred only as a single liquid phase in the shale reservoir position. When burial depth and temperature increased to 3500 m and 152 °C respectively (200 ma) (Figs. 3 and 12E), the reservoir liquid phase became gassier and *GORs* started to increase rapidly due to the beginning of secondary cracking of oil compounds (Figs. 3, 10 and 12 E). Black oil has evolved to volatile oil but P_b (290 bar) was still lower than P_r. The single oil phase under shale reservoir conditions was therefore maintained.

Later, at Early Jurassic times (187 ma) temperatures increased to 165 °C for burial depth around 4000 m (Figs. 3 and 12 F). Assuming that all compounds stayed in place, fluid in the reservoir changed from undersaturated liquid (volatile oil) into undersaturated gas (wet gas). P_b was reduced to ~200 bars, and started to decrease continuously from an increasing process from A to E. In that case, a single gas phase could change into a gas-oil phases when 200 bar of P_b reached. With a continuous increase of burial depth and temperature in the Middle–Late Jurassic, *GORs* climbed rapidly (Fig. 10) by secondary cracking of the remaining oil compounds. P_b decreased to lower than 100 bar while P_r increased to ~600 bar by the end of the Jurassic (Figs. 3 and 12, G and H). Fluids under the shale reservoir conditions occurred as a gas phase predominated by methane with only minor amounts of light hydrocarbons being present. Thus, although Lower Cambrian shale in the UYP has been significantly uplifted since Cretaceous (Fig. 3 I), only the vapour phase (dry gas) reservoir could form within this formation.

Bubble point pressures were significantly below corresponding reservoir pressures in the whole burial process for each stage (Figs. 3 and 12). As a result from constant burial from Permian to Jurassic times, the formation experienced the highest temperatures of ~220 °C by the end of the Jurassic, and lasted for 60-70 ma in a high temperature zone (>200 °C) (from G to I in Fig. 3). When organic matter suffers such high temperatures over a long time span, hydrocarbons formed in the shale reservoir can be only gases regardless how the pressure changes (Fig. 12 G and H).

Thus, only a single phase would have existed in the Lower Cambrian shale assuming hydrocarbons were completely preserved in the source rock within an unconventional system. A liquid phase (black oil and volatile oil) would have dominated during the primary generation process and a gas phase (wet gas and dry gas) during the secondary generation process. However, phase separation of the fluid into an oil leg and a gas cap would have occurred if the liquid petroleum had migrated during early maturation stages to a shallower, for example conventional reservoir in which bubble point pressure might have been higher than the corresponding reservoir pressure.

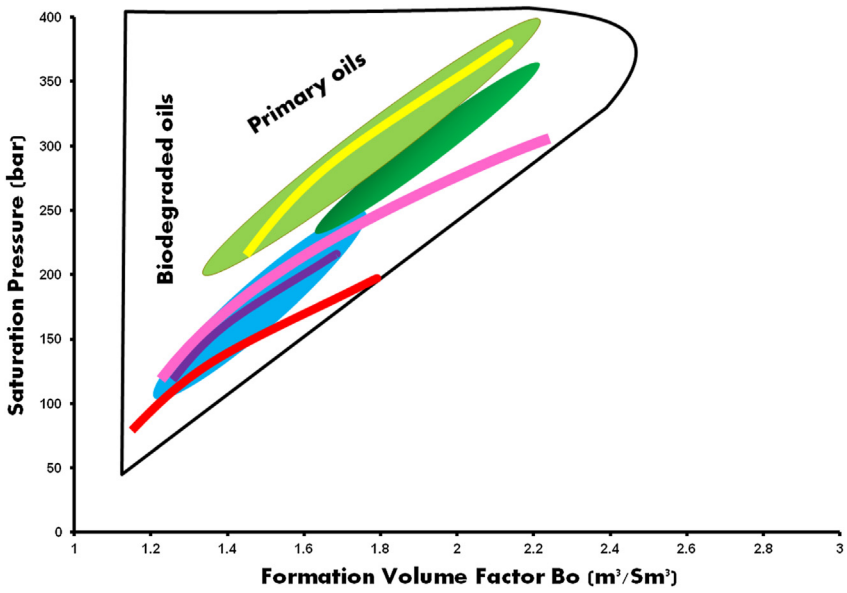

Figure 11. Predicted P_{sat} and B_o for a heating rate of 1.5 °C/ma. *Ellipses are the ranges of natural oils from the Central Graben* (*light green*) (di Primio and Neumann, 2008), *Viking Graben* (*green*) (Bhullar et al., 2003) *and Tampen Spur* (*light blue*) (di Primio et al., 1998) in the Northern Sea, Norway (from the top down). Curves are the predicted ranges of natural oils in the Central Graben (yellow), Lower Cambrian shale in the UYP (pink), natural oils in the Tampen Spur (purple) (di Primio and Skeie, 2004) *and Bakken shale* (*USA*, *red*) (Kuhn et al., 2010) (*from the top down*). (For interpretation of the references to colour in this figure legend, the reader is referred to the web version of this article.)

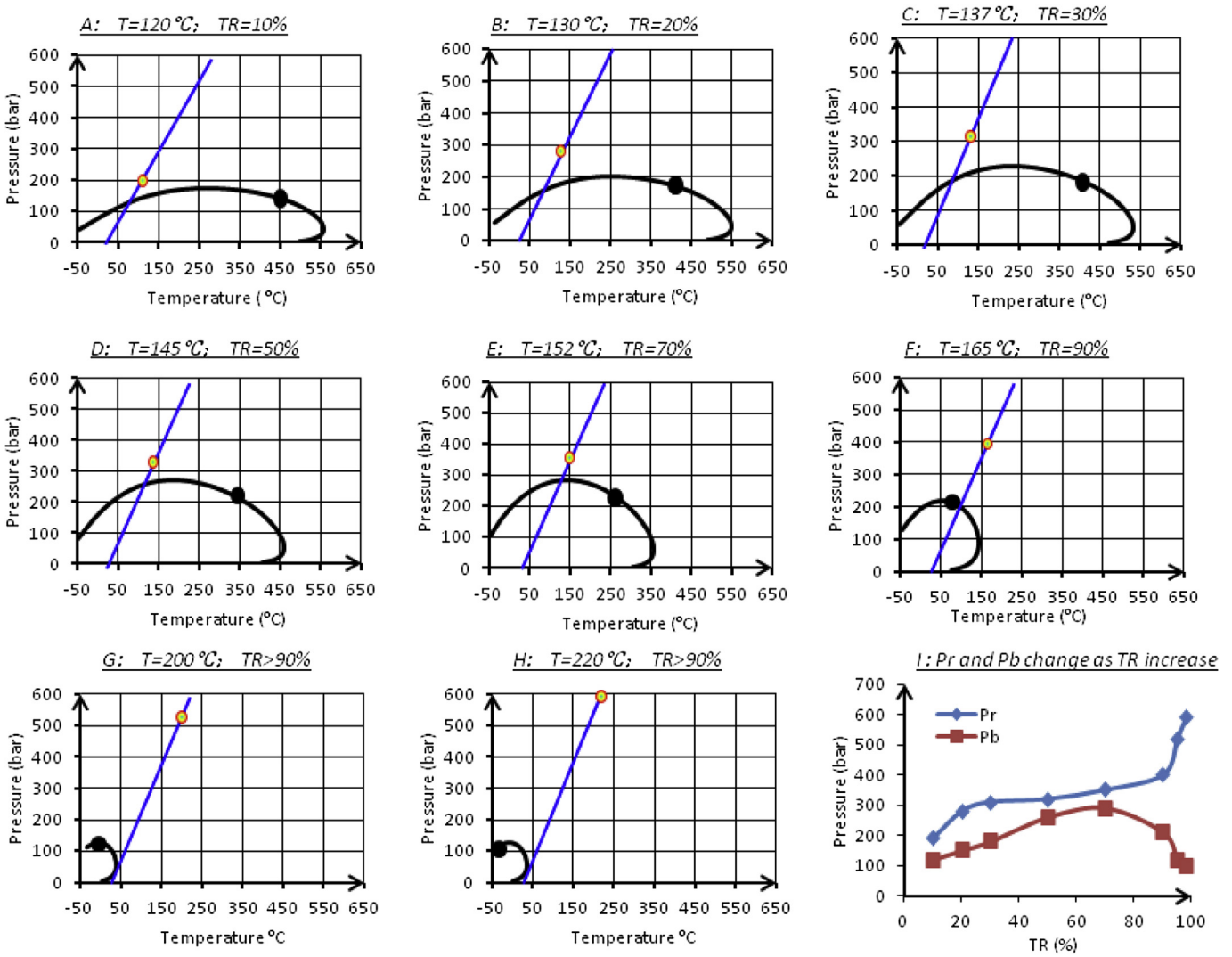

Figure 12. Phase behaviour evolution with burial depth and temperature increasing of Lower Cambrian shale in the UYP. Diagonals are the temperature–pressure gradients in reservoir conditions; Points on the diagonal are the reservoir conditions in given times; Curves are the phase envelopes; Points on the envelope are bubble points; Plots A-H are corresponding to the six reservoir positions in Figure 3.

6. Conclusions

Geological temperature-depth history of a well located in the UYP showed that the Lower Cambrian shale succession was influenced strongly by uplifts between the end of the Silurian and Carboniferous, which resulted in erosion of younger sediment packages. The sedimentation generally continued from Permian to Jurassic, with an interruption by a short uplift phase during Middle to Late Permian times. The deepest burial depth of 6000 m with a maximum temperature of 220 °C occurred during the Late Jurassic. From then on, the UYP entered into the third uplift period commencing in the Cretaceous. At present, organic matter in Lower Cambrian shale contains normally between 5 and 10% TOC which is overmature. It possesses only very low remaining petroleum generation potential, but huge amounts of hydrocarbons must have been generated during geological history.

Based on the adjacent tectonic position and comparable Cambrian geology of North Australia and South China, an immature Cambrian Shale sample from the Georgina Basin was used to investigate the petroleum generation kinetics of the Lower Cambrian shale in the UYP, as well as petroleum phase evolution within an unconventional shale reservoir in this formation. The analysis on source rock characteristics suggested a type II kerogen and an organofacies inferring paraffinic–naphthenic–aromatic low wax oil generation. Hydrocarbon generation can be described by a single frequency factor of $A = 8.429E + 14$ 1/sec and an activation energy distribution ranging from 44 to 67 kcal/mol. The main activation energy of 56 kcal/mol is higher than commonly assumed oil and gas formation from marine, clastic source rocks, and indicated presence of marine but highly stable, sulphur-poor organic matter in the Cambrian shale. The onset temperature of hydrocarbon generation ($TR = 10\%$) is ~120 °C, while end of generation ($TR = 90\%$) can be expected for temperatures around 165 °C for a geological heating rate of 1.5 °C/Ma.

Phase behaviour properties for onset and end of bulk hydrocarbon generation from kerogen can be described by a *GOR* of 63 Sm^3/Sm^3, P_{sat} of 101 bar and B_o of 1.2 m^3/Sm^3 at 10% *TR*, and a *GOR* of 176 Sm^3/Sm^3, P_{sat} of 189 bar and B_o of 1.61 m^3/Sm^3 at 90% *TR*. Onset occurred in the Middle Triassic (241 ma) at burial depths around 2000 m for temperature close to 120 °C. Before 203 ma, for temperatures <145 °C, burial depth <3300 m, and *TR* <50%, phase behaviour of generated black oil was defined by primary product evolution. Secondary cracking of oil to gas predominated with increasing burial depth and temperature in Middle–Late Jurassic times. Kerogen conversion was completed in the Early Jurassic (187 ma) at depths close to 4000 m and temperatures around 165 °C.

In the Lower Cambrian shale reservoir, bubble point pressure was much lower than the reservoir pressure during the whole maturation process. Unconventional shale resources can therefore only be present as a single phase, and were dominated by a single liquid phase (black oil and volatile oil) during the primary generation process and a single vapour phase (wet gas and dry gas) during secondary cracking processes.

Limitations of the model exist with respect to hydrocarbon expulsion since generated hydrocarbons were regarded as retained petroleum. In addition, the predicted petroleum physical properties rely on local geological background and original kerogen type, hence, the applicability of the conclusions presented in this paper has to be considered prudently when apply to other unconventional shale system.

Acknowledgement

The authors thank Ferdinand Perssen (GFZ-Potsdam) for his technical assistance and Statoil for funding and publication permission. We are grateful to all anonymous reviewers for their constructive comments and suggestions.

Appendix

GOR (Sm^3/Sm^3) (gas oil ratio) is the ratio of total gas hydrocarbons (C_{1-5}) and total liquid hydrocarbons (C_{6+}) at standard surface conditions.

$\boldsymbol{B_o}$ (m^3/Sm^3) is the formation volume factor, which is the ratio of reservoir liquid volume to surface liquid volume.

$\boldsymbol{P_{sat}}$ (bar) is the saturation pressure, which is the reservoir pressure occurring when the system changes from a one-phase system to a two-phase system or vice versa.

$\boldsymbol{P_r}$ (bar) is the reservoir pressure.

$\boldsymbol{P_b}$ (bar) is the bubble point pressure.

References

Ambrose, G.J., Kruse, P.D., Putnam, P.E., 2001. Geology and hydrocarbon potential of the southern Georgina Basin, Australia. APPEA Journal 41 (1), 139–163.

Ambrose, G.J., Putnam, P.E., 2005. Carbonate ramp facies and oil plays in the Middle–Late Cambrian, southern Georgina Basin, Australia. In: Munson, T.J., Ambrose, G.J. (Eds.), Proceedings of the Central Australian Basins Symposium (CABS). Northern Territory Geological Survey, Alice Springs, Northern Territory, Australia, pp. 236–253.

Behar, F., Vandenbroucke, M., Tang, Y., Marquis, F., Espitalie, J., 1997. Thermal cracking of kerogen in open and closed systems: determination of kinetic parameters and stoichiometric coefficients for oil and gas generation. Organic Geochemistry 26 (5–6), 321–339.

Bhullar, A.G., di Primio, R., Karlsen, D.A., Gustin, D.-P., 2003. Determination of the timing of petroleum system events using petroleum geochemical, fluid inclusion, and PVT data: an example from the rind discovery and Frøy Field, Norwegian North Sea. In: Düppenbecker, S., Marzi, R. (Eds.), Multidimensional Basin Modeling, AAPG/Datapages Discovery Series No. 7, pp. 123–135.

Boreham, C.J., Ambrose, G.J., 2007. Cambrian petroleum systems in the southern Georgina Basin, Northern Territory, Australia. In: Munson, T.J., Ambrose, G.J. (Eds.), Proceedings of the Central Australian Basins Symposium (CABS). Northern Territory Geological Survey, Alice Springs, Northern Territory, Australia, pp. 254–281.

Braun, R.L., Burnham, A.K., 1992. PMOD: a flexible model of oil and gas generation, cracking, and expulsion. Organic Geochemistry 19 (1–3), 161–172.

Burnham, A.K., Braun, R.L., Gregg, H.R., Samoun, A.M., 1987. Comparison of methods for measuring kerogen pyrolysis rates and fitting kinetic parameters. Energy & Fuels 1 (6), 452–458.

Cheng, K., Wang, S., Dong, D., Huang, J., Li, X., 2009. Accumulation conditions of shale gas reservoirs in the lower Cambrian Qiongzhusi formation, the upper Yangtze region. Natural Gas Industry 29 (5), 40–44.

Dai, J., Ni, Y., Zou, C., Tao, S., Hu, G., Hu, A., Yang, C., Tao, X., 2009. Stable carbon isotopes of alkane gases from the Xujiahe coal measures and implication for gas-source correlation in the Sichuan Basin, SW China. Organic Geochemistry, 638–646.

Dai, J., Pei, X., Qi, H., 1992. China Natural Gas Geology, vol. I. Petroleum Industry Press, p. 298.

di Primio, R., Dieckmann, V., Mills, N., 1998. PVT and phase behaviour analysis in petroleum exploration. Organic Geochemistry 29 (1–3), 207–222.

di Primio, R., Horsfield, B., 2006. From petroleum-type organofacies to hydrocarbon phase prediction. AAPG Bulletin 90 (7), 1031–1058.

di Primio, R., Neumann, V., 2008. HPHT reservoir evolution: a case study from Jade and Judy fields, Central Graben, UK North Sea. International Journal of Earth Sciences 97 (5), 1101–1114.

di Primio, R., Skeie, J.E., 2004. Development of a Compositional Kinetic Model for Hydrocarbon Generation and Phase Equilibria Modelling: a Case Study from Snorre Field, Norwegian North Sea. In: Geological Society, London, Special Publications, vol. 237 (1), pp. 157–174.

Dieckmann, V., Schenk, H.J., Horsfield, B., Welte, D.H., 1998. Kinetics of petroleum generation and cracking by programmed-temperature closed-system pyrolysis of Toarcian Shales. Fuel 77 (1–2), 23–31.

Dong, D., Cheng, K., Wang, Y., Li, X., Wang, S., Huang, J., 2010. Forming condition and characteristics of shale gas in the lower Paleozoic of the upper Yangtze region, China. Oil & Gas Geology 31 (3), 288–299.

Editorial Committee Division of Sichuan Oil & Gas field, E., 1989. Sichuan Oil & Gas Field. In: Petroleum Geology of China, vol. 10. Petroleum Industry Press, Beijing, p. 516.

EIA, 2011. World Shale Gas Resources: an Initial Assessment of 14 Regions Outside the United States. U.S. Department of Energy, Washington. DC.

Espitalié, J., Marquis, F., Barsony, I., 1984. Geochemical logging. In: Voorheers, K.T. (Ed.), Analytical Pyrolysis Techniques and Applications. Butterworth, London, pp. 276–304.
Haines, P.W., Hand, M., Sandiford, M., 2001. Palaeozoic synorogenic sedimentation in central and northern Australia: a review of distribution and timing with implications for the evolution of intracontinental orogens. Australian Journal of Earth Sciences 48 (6), 911–928.
Hao, F., Guo, T., Zhu, Y., Cai, X., Zou, H., Li, P., 2008. Evidence for multiple stages of oil cracking and thermochemical sulfate reduction in the Puguang gas field, Sichuan Basin, China. AAPG Bulletin 92 (5), 611–637.
Hartgers, W.A., Damsté, J.S.S., de Leeuw, J.W., 1994. Geochemical significance of alkylbenzene distributions in flash pyrolysates of kerogens, coals, and asphaltenes. Geochimica et Cosmochimica Acta 58 (7), 1759–1775.
Horsfield, B., 1989. Practical criteria for classifying kerogens: some observations from pyrolysis-gas chromatography. Geochimica et Cosmochimica Acta 53 (4), 891–901.
Horsfield, B., Disko, U., Leistner, F., 1989. The micro-scale simulation of maturation: outline of a new technique and its potential applications. Geologische Rundschau 78 (1), 361–373.
Huang, J., Chen, S., Song, J., Wang, L., Gou, X., Wang, T., Dai, H., 1997. Hydrocarbon source systems and formation of gas fields in Sichuan Basin. Science in China Series D: Earth Sciences 40 (1), 32–42.
Jia, D., Wei, G., Chen, Z., Li, B., Zeng, Q., Yang, G., 2006. Longmen Shan fold-thrust belt and its relation to the western Sichuan Basin in central China: new insights from hydrocarbon exploration. AAPG Bulletin 90 (9), 1425–1447.
Korsch, R.J., Huazhao, M., Zhaocai, S., Gorter, J.D., 1991. The Sichuan basin, southwest China: a Late Proterozoic (Sinian) petroleum province. Precambrian Research 54 (1), 45–63.
Kuhn, P., Primio, R.D., Horsfield, B., 2010. Bulk composition and phase behaviour of petroleum sourced by the Bakken Formation of the Williston Basin. In: Geological Society, London, Petroleum Geology Conference Series, vol. 7, pp. 1065–1077.
Li, Z.-X., Zhang, L., Powell, C.M., 1995. South China in Rodinia: part of the missing link between Australia–East Antarctica and Laurentia? Geology 23 (5), 407–410.
Li, Z.X., Li, X.H., Kenny, P.D., Wang, J., Zhang, S., Zhou, H., 2003. Geochronology of Neoproterozoic syn-rift magmatism in the Yangtze Craton, South China and correlations with ther continents: evidence for a mantle superplume hat broke up Rodinia. Precambrian Research 122, 85–109.
Liang, D., Guo, T., Chen, J., Bian, L., Zhao, Z., 2008. Some progresses on studies of hydrocarbon generation and accumulation in marine sedimentary region, southern China (part 1): distribution of four suits of regional marine source rocks. Marine Origin Petroleum Geology 13 (3), 1–16.
Liang, D., Guo, T., Chen, J., Bian, L., Zhao, Z., 2009. Some progresses on Studies of hydrocarbon generation and accumulation in marine sedimentary region, southern China (part 2): geochemical characteristics of four suits of regional marine source rocks, South China. Marine Origin Petroleum Geology 14 (1), 1–15.
Long, P., Zhang, J., Li, Y., Tang, X., Cheng, L., Liu, Z., Han, S., 2012. Reservoir-forming conditions and strategic select favorable area of shale gas in the Lower Paleozoic of Chongqing and its adjacent areas. Earth Science Frontiers 19 (2), 221–243.
Ma, Y., Cai, X., Zhao, P., Luo, Y., Zhang, X., 2010. Distribution and further exploration of the large-medium sized gas fields in Sichuan Basin. Acata Petrol Ei Sinica 31 (3), 347–354.
Ma, Y., Guo, X., Guo, T., Huang, R., Cai, X., Li, G., 2007. The Puguang gas field: new giant discovery in the mature Sichuan Basin, southwest China. AAPG Bulletin 91, 627–643.
Ma, Y.S., Mu, C.L., Guo, X.S., Tan, Q.Y., Yu, Q., 2006. Characteristic and framework of the Changxingian sedimentation in the northeastern Sichuan Basin (in Chinese with English abstract). Geological Review 52 (1), 25–39.
Meng, Q.-R., Wang, E., Hu, J.-M., 2005. Mesozoic sedimentary evolution of the northwest Sichuan basin: implication for continued clockwise rotation of the South China block. Geological Society of America Bulletin 117 (3–4), 396–410.
Muscio, G.P.A., Horsfield, B., Welte, D.H., 1994. Occurrence of thermogenic gas in the immature zone—implications from the Bakken in-source reservoir system. Organic Geochemistry 22 (3–5), 461–476.
National Bureau of Statistics, P., Energy Bureau, P. (Eds.), 1991–2010. China Energy Statistical Yearbook. China Statistics Press, Beijing.
Plesch, A., Shaw, J.H., Kronman, D., 2007. Mechanics of low-relief detachment folding in the Bajiaochang field, Sichuan Basin, China. AAPG Bulletin 91 (11), 1559–1575.
Schenk, H.J., Di Primio, R., Horsfield, B., 1997. The conversion of oil into gas in petroleum reservoirs. Part 1: comparative kinetic investigation of gas generation from crude oils of lacustrine, marine and fluviodeltaic origin by programmed-temperature closed-system pyrolysis. Organic Geochemistry 26 (7–8), 467–481.
Scotese, C.R., 2009. Late Proterozoic Plate Tectonics and Palaeogeography: A Tale of Two Supercontinents, Rodinia and Pannotia. In: Geological Society, London, Special Publications, vol. 326 (1), pp. 67–83.
Scotese, C.R., McKerrow, W.S., 1990. Revised World Maps and Introduction. In: Geological Society, London, Memoirs, vol. 12 (1), pp. 1–21.
Steiner, M., Li, G., Qian, Y., Zhu, M., Erdtmann, B.-D., 2007. Neoproterozoic to Early Cambrian small shelly fossil assemblages and a revised biostratigraphic correlation of the Yangtze Platform (China). Palaeogeography, Palaeoclimatology, Palaeoecology 254 (1–2), 67–99.
Tan, J., Horsfield, B., Mahlstedt, N., Zhang, J., Boreham, C.J., Hippler, D., van Graas, G., Tocher, B.A., 2013. Geological and geochemical characterization of the Upper Sinian and Lower Paleozoic black shales in the Upper Yangtze Platform, South China: implications for shale gas potential (in press).
Tegelaar, E.W., Noble, R.A., 1994. Kinetics of hydrocarbon generation as a function of the molecular structure of kerogen as revealed by pyrolysis-gas chromatography. Organic Geochemistry 22 (3–5), 543–574.
Volk, H., George, S.C., Kempton, R.H., Liu, K., Ahmed, M., Ambrose, G.J., 2007. Petroleum migration in the Georgina Basin: evidence from the geochemistry of oil inclusions and bitumens. In: Munson, T.J., Ambrose, G.J. (Eds.), Proceedings of the Central Australian Basins Symposium (CABS). Northern Territory Geological Survey, Alice Springs, Northern Territory, Australia, pp. 282–303.
Wang, L., Zou, C., Deng, P., Chen, S., Zhang, Q., Xu, B., Li, H., 2009a. Geochemical evidence of shale gas existed in the lower Paleozoic Sichuan basin. Natural Gas Industry 29 (5), 59–62.
Wang, S., Chen, G., Dong, D., Yang, G., Lu, Z., Xu, Y., Huang, Y., 2009b. Accumulation conditions and exploitation prospect of shale gas in the lower Paleozoic Sichuan basin. Natural Gas Industry 29 (5), 51–58.
Wanglu, J., Ping'an, P., Chiling, Y., Zhongyao, X., 2007. Source of 1,2,3,4-tetramethylbenzene in asphaltenes from the Tarim Basin. Journal of Asian Earth Sciences 30 (5–6), 591–598.
Xu, M., Zhu, C., Tian, Y., Rao, S., Hu, S., 2011. Borehole temperature logging and characteristics of subsurface temperature in the Sichuan Basin. Chinese Journal Geophysics 54 (4), 1052–1060.
Zhang, J., Nie, H., Xu, B., Jiang, S., Zhang, P., Wang, Z., 2008. Geological condition of shale gas accumulation in Sichuan basin. Natural Gas Industry 28 (2), 151–156.
Zhu, C., Xu, M., Yuan, Y., Zhao, Y., Shan, J., He, Z., Tian, Y., Hu, S., 2010. Palaeogeothermal response and record of the effusing of Emeishan basalts in Sichuan basin. Chinese Science Bulletin 55 (6), 474–482.
Zou, C., Dong, D., Wang, S., Li, J., Li, X., Wang, Y., Li, D., Cheng, K., 2010. Geological characteristics and resource potential of shale gas in China. Petroleum Exploration and Development 37 (6), 641–653.
Zou, C., Dong, D., Yang, H., Wang, Y., Huang, J., Wang, S., Fu, C., 2011. Conditions of shale gas accumulation and exploration practices in China. Natural Gas Industry 31 (12), 26–39.